Structural Eng./Earthquake Eng., JSCE, Vol. 14, No. 2, 139s—147s, 1997 July
(J. Struct. Mech. Earthquake Eng., JSCE, No. 570/ I —40)

DETERMINISTIC SEISMIC HAZARD MAP OF JAPAN FROM INLAND MAXIMUM CREDIBLE EARTHQUAKES FOR ENGINEERING

Tsutomu NISHIOKA[1] and Lalliana MUALCHIN[2]

[1]Member of JSCE, Engineer, Hanshin Expressway Public Corporation (4-1-3 Kyutaro-machi, Chuo-ku, Osaka 541, Japan)
[2]Ph. D., Senior Engineering Seismologist, California Department of Transportation (1801 30th Street, Sacramento, CA 94274-0001, U.S.A.)

A deterministic seismic hazard map of Japan using the concept of maximum credible earthquakes (MCE's) is developed for engineering. Seismogenic mapped faults on land in Japan[1)], which may produce a significant earthquake, are used for seismic sources. An appropriate attenuation relationship of peak rock accelerations (PRA's) for this analysis is selected after comparing five published attenuation studies. The horizontal PRA's are obtained by applying the estimated MCE magnitude to the attenuation relationship. The median PRA contours for 0.7g, 0.5g, 0.3g, and 0.1g (g: acceleration due to gravity) levels are shown in the seismic hazard map.

Key Words : deterministic seismic hazard map, seismogenic fault, maximum credible earthquake, peak rock acceleration

1. INTRODUCTION

The Hyogoken-Nanbu earthquake or the Great Hanshin earthquake of January 17, 1995 caused disastrous damage in the vicinity of Kobe. This is the first destructive earthquake that has hit one of the most urbanized areas of Japan since the 1923 Great Kanto earthquake[2)]. This case proved that an inland earthquake with a shallow source centered close to modern cities can be fatal. Therefore, much attention should be paid to shallow earthquakes from active faults near or beneath populated areas.

In one of the important seismic hazard evaluations using MCE's, Omote at el.[3)] proposed the horizontal peak ground velocity (PGV) from MCE's as a maximum ground motion parameter at a nuclear power plant site. They produced a seismic zoning map of Japan based on the MCE magnitudes derived from historical earthquake records and seismotectonic structures. The MCE magnitudes of active faults were estimated according to fault length, fault slip rate, and earthquake recurrence. The horizontal PGV is obtained from the empirical relationship between earthquake magnitude and the distance from the site to the geometrical center of fault rupture, which is assumed to be the center of the earthquake energy release. The validity of this relationship is limited to larger epicentral distances. It gives too large values in the near-field region. Thus, a correction is needed at sites close to active faults.

In another effort to approximate the seismic hazard of Japan by the MCE concept, Matsuda[1)] grouped active faults on land into seismogenic faults which can produce an independent, large earthquake. He estimated the MCE magnitude in the JMA scale for each seismogenic fault by using an empirical relationship between fault length and magnitude. He provided a single MCE magnitude for each seismotectonic province in a seismic zoning map of Japan according to historical earthquake records and the estimated MCE magnitudes. However, a single magnitude in a particular province is not detailed enough to evaluate site-specific engineering seismic loads.

In a seismic hazard estimation of Japan, Kameda and Okumura[4)] divided Japan and its vicinity into 22 regions and calculated earthquake occurrence rates for each region using information combined historical earthquakes and active faults. They

estimated the number of earthquakes in a certain period, the magnitude, and the location of epicenter on the basis of simulation results and developed contours of peak ground acceleration. This probabilistic method gives low earthquake occurrence rates to the regions with scarce historical earthquake data and small slip-rate faults.

In a study of California, another highly seismic region, Mualchin and Jones[5] presented a deterministic seismic hazard map with peak accelerations from MCE's on rock and stiff-soil sites for use in engineering. They selected seismogenic faults for seismic sources with the following criteria: 1) geologic age of last displacement is late Quaternary or younger; 2) length of fault is 10 km or more; 3) location of fault is in California and adjacent areas; and 4) historic earthquakes occurred along the fault. They estimated the MCE magnitude (moment magnitude) for each fault by using a correlation between fault parameters (fault length and fault area) and magnitude, or the largest historical event that have occurred along a particular fault. They constructed the median PRA contours based on the MCE's and a suitable attenuation relationship. When the acceleration effects to structures become significantly larger in short periods, particularly in the near-field region, PRA is a useful index to express earthquake ground motions for engineering purposes. This type of ground shaking map has been used to obtain seismic loads in the bridge design specifications of the California Department of Transportation (Caltrans) since shortly after the 1971 San Fernando earthquake. The experience and application for more than two decades by Caltrans have proved that this map is reasonable and practical for assessing seismic loads for bridge engineering in California.

In a probabilistic seismic hazard analysis based on earthquake recurrence, the results from low probability faults sometimes got upset by the occurrence of earthquakes, such as the 1992 Landers, the 1994 Northridge, and the 1995 Great Hanshin earthquakes. The deterministic approach, however, avoids this problem. In the deterministic map, active faults supposedly having long recurrence or low probability are taken into consideration. The resultant ground motions from the deterministic MCE's are conservative and therefore appropriate for critical structures and for public safety. It should be noted that understanding of earthquake recurrence are in an active but still premature stage of scientific inquiry.

In this study, shallow inland seismic sources which can cause destructive earthquakes like the Great Hanshin earthquake are considered. As this type of seismic source is dominant in California, a seismic hazard map from MCE's on the Japanese islands is developed following the basic procedures of Mualchin and Jones[5]. Comparison of design seismic forces for a single column bent for Caltrans' and Japanese highway bridge specifications is also presented.

2. SEISMOGENIC FAULTS AS SEISMIC SOURCES

Matsuda[1] grouped all the active or Quaternary faults on land in Japan into seismogenic faults that can produce independent, significant earthquakes repeatedly. The active fault data are from Active Faults in Japan[6], a comprehensive evaluation of active faults in and adjacent to Japan. His criteria for grouping are as follows:

1) An isolated active fault with more than 10 km length with no other active faults within 5 km of the fault.

2) A group of faults which are located on a straight line. The distance between the ends of nearby faults is less than 5 km.

3) A group of faults which run parallel to each other with less than 5 km intervals.

4) A subsidiary fault with a different trend from the nearby principal strand of the main fault zone. The distance between the middle point of the subsidiary fault and the main fault is more than 5 km.

The reasons for using 5 km as the critical distance with respect to grouping faults in proximity are that 1) the widths of the main fault zones in historical intra-plate earthquakes are within 5 km and that 2) the distances between the middle point of the subsidiary faults and the principal strand of the main fault zone are less than 5 km.

Matsuda divided Japanese land and sea areas into seismotectonic provinces based on the tectonic structure of the island arc system, the distribution of active faults, and the historically large earthquakes. Then he tabulated seismogenic faults

for each province. This study adopts seismogenic faults in Matsuda's tables. Some modification in measuring fault lengths is necessary due to the revision of the Active Faults in Japan[7]. **Fig.1** shows 236 seismogenic faults on Japanese islands.

Deep seated faults are not incorporated here, but they should be considered in the future as information on the geometry of these faults become available. The source of the 1923 Great Kanto earthquake is not included because of lack of the source geometry, and the region around that earthquake should note this limitation. Also, effects from the subduction zone should be considered in the future, particularly for long period seismic waves. These would be important for structures with long periods.

3. ESTIMATION OF MAXIMUM CREDIBLE EARTHQUAKE (MCE) MAGNITUDE

MCE is defined as the largest earthquake that appears capable of occurring under the presently known tectonic framework[5]. The longer the surface fault rupture in the earthquake, the larger the magnitude of the event[8]. Similarly, Matsuda[9] assumed that the longer active fault can generate the larger earthquakes and developed an empirical relationship between length of surface fault trace and magnitude in the JMA scale. To derive the relationship, he used the past 100 year historical records of earthquakes in the Japanese islands. His relationship is,

$$\log_{10} L = 0.6\, M_j - 2.9 \qquad (1)$$

where, L (km) is the surface fault length and M_j is the JMA magnitude.

The MCE magnitude of each seismogenic fault is calculated by Eq.(1) and rounded to the nearest quarter of a magnitude unit between 6.5 and 8.0. The approximation to a quarter magnitude is a practical consideration to quantify seismogenic faults in a reasonable manner. The lowest magnitude 6.5 corresponds to a 10 km long fault. It should be recognized that less than 6.5 earthquakes could happen anywhere in the Japanese islands from the view point of Japanese seismotectonic structure[3]. Matsuda[1] excluded exceptionally long faults from estimating MCE's, because he thought

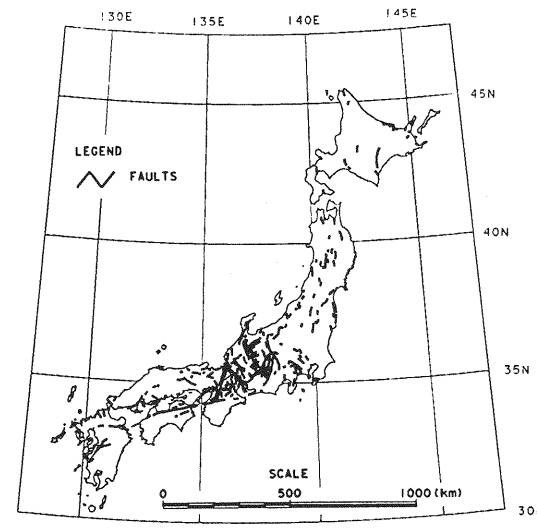

Fig.1 Seismogenic faults on land in Japan [1]

that the entire length would not move during an earthquake. Rather, these long faults may move as shorter seismogenic segments as judged from historical earthquakes. In this study, after Eq.(1) is applied to all seismogenic faults, an upper limit of the MCE magnitude is set at 8.0 for practical application.

4. SELECTION OF ATTENUATION RELATIONSHIP

Five published attenuation relationships are compared. In this study, the larger of peak ground accelerations (PGA's) in g's from two horizontal components on rock sites, the shortest distance (km) to surface projection of fault rupture, and the JMA magnitude are used as attenuation parameters. The stiffer the bedrock, the more precise the predicted PGA. Note that the ground conditions in Japan, however, are generally softer than in California. The rock is defined here as the base layer with shear wave velocity, Vs > 300 m/s which corresponds to Type I (Rock) in the classification of the JMA stations. Due to the differences among the definitions of PGA, distance, magnitude, and soil classification in the five attenuation equations, some assumptions are necessary for comparison. The five attenuation studies are discussed below.

Campbell[10] gave the following equation for the near-field attenuation,

$$PGA = 0.0159 \exp(0.868\ M)\ [\ R + 0.0606\exp(0.700\ M)\ ]^{-1.09} \quad (2)$$

where, PGA (g) is the mean of the peak ground acceleration from the two horizontal components, M is the Richter local magnitude for M<6 or the surface-wave magnitude for M≥6, and R (km) is the shortest distance from the fault rupture zone to the site. Eq.(2) is applicable to worldwide regions, to 5.0<M<7.7, to R<50 km, and to rock or deeper than 10 m soil sites[11].

Annaka and Nozawa[12] derived the following relationship for ground sites with Vs > 300 m/s.

$$\log_{10} PGA = 0.627\ M_j + 0.00671\ H - 2.212 \log_{10} D + 1.711 \quad (3)$$

$$D = R + 0.35 \exp(0.65 M_j) \quad (4)$$

where, PGA (cm/sec^2) is the mean of the peak ground acceleration from two horizontal components, M_j is the JMA magnitude, R (km) is the shortest distance to the fault rupture, and H (km) is the depth to the point on the fault where R is measured.

Fukushima and Tanaka[13] developed the following equation applicable to the near-source region in Japan by supplementing it with near-source data in the United States.

$$\log_{10} PGA = 0.41\ M_s - \log(R + 0.032 \cdot 10^{0.41 M_s}) - 0.0034\ R + 1.30 \quad (5)$$

where, PGA (cm/sec^2) is the mean of the peak acceleration from two horizontal components, R (km) is the shortest distance between the site and the fault rupture, and M_s is the surface-wave magnitude. Average PGA for rock sites (Type I) is 60% of the value predicted from Eq.(5).

Boore et al.[14] presented another equation for site class B, where the average Vs is between 360 and 750 m/s.

$$\log_{10} PGA = -0.038 + 0.216\ (M_w - 6) - 0.777 \log_{10} r + 0.158 \quad (6)$$

$$r = (D^2 + h^2)^{(1/2)} \quad (7)$$

where, PGA (g) is the larger of the peak acceleration from two horizontal components, M_w is the moment magnitude, D (km) is the shortest distance to surface projection of the fault rupture, and h is a fictitious depth that is determined by regression analysis, which is 5.48 km in this case.

Finally, Molas and Yamazaki[15] developed an attenuation equation applicable to subduction zone sources as well by using earthquakes with depths up to 200 km and modified it slightly by adding the Great Hanshin Earthquake data[16].

$$\log_{10} PGA = 0.184 + 0.482 M_j - \log R - 0.00149 R + 0.00315 H + c_i^a \quad (8)$$

where, PGA (cm/sec^2) is the larger of the peak acceleration from two horizontal components, M_j is the JMA magnitude, R (km) is the shortest distance to the fault rupture, H (km) is the depth to the point on the fault where R is measured, and c_i^a is a recording station coefficient. The mean coefficient for the rock sites (Type I) is -0.055.

In order to compare the five relationships directly, the fault rupture is assumed to be a vertical plane with 5 km depth (**Fig.2**). The mean PGA from two horizontal components is adjusted to the larger PGA by a factor of 1.11 in accordance with the mean ratio of the two values[17], which is applied to Eqs.(2), (3), and (5). The surface-wave magnitudes and the moment magnitudes are converted to the JMA magnitudes in Eqs.(2), (5), and (6) according to the relationships given by Utsu[18].

Figs.3(a)-(d) show comparison of attenuation relationships for M_j = 6.5, 7.0, 7.5 and 8.0, respectively. Comparison is to be made in the range from 5 to 100 km. In less than 5 km, there is not much reliability in the attenuation relationships owing to only a few near-field data available. In more than 100 km, PRA's drop to the negligible level from the engineering standpoint.

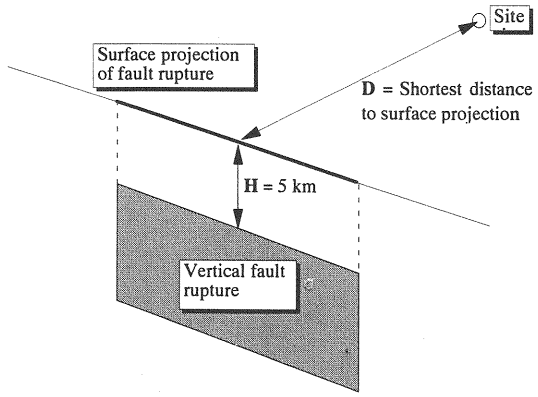

Fig.2 Fault model used in comparison of attenuation relationships

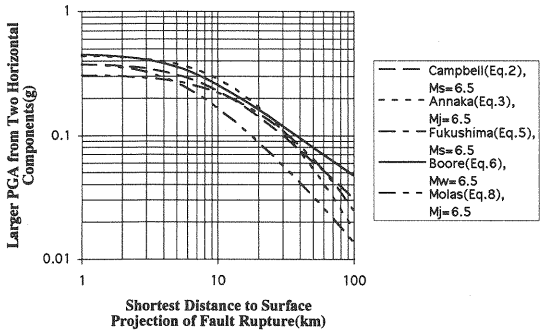

Fig.3(a) Comparison of attenuation relationships (M_j=6.5)

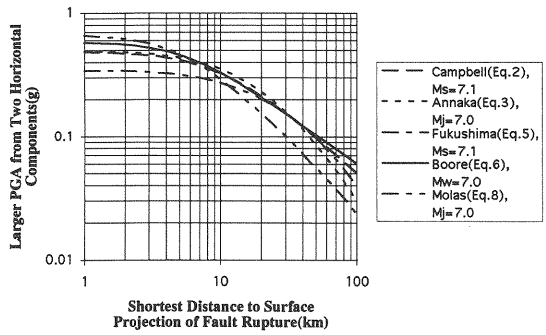

Fig.3(b) Comparison of attenuation relationships (M_j=7.0)

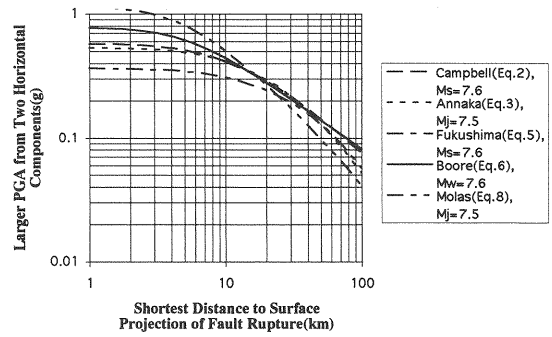

Fig.3(c) Comparison of attenuation relationships (M_j=7.5)

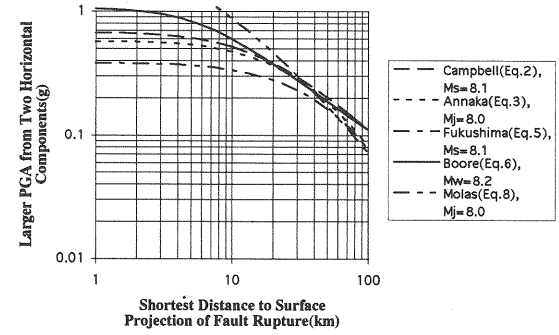

Fig.3(d) Comparison of attenuation relationships (M_j=8.0)

A reasonably conservative PRA is desirable, and Eq.(6) results in relatively high PRA's from M_j = 6.5 through 8.0. Thus, Eq.(6) is chosen for this study. Although Eq.(8) results in the highest PRA's within about 10 km for M_j = 7.5 and 8.0, it is not used here because of scarcity of near-field data in deriving Eq.(8) and the unrestrained characteristic near the fault rupture. There should be some saturation of peak ground acceleration very close to the fault rupture. Adopting average or envelope curves from the five equations is avoided, because each equation does not use distinct earthquake data, but share some of the records. The weight of the earthquake data in each equation should not be changed.

Table 1 shows the adopted attenuation relationship for each quarter of MCE's from 6.5 up to 8.0, derived from Eq.(6).

Table 1 Attenuation Relationship, Eq(6)

PRA		Shortest Distance to Surface Projection of Fault Rupture(km)			
		0.1g	0.3g	0.5g	0.7g
Mj	Mw				
6 1/2	6.5	37.7	7.5	-	-
6 3/4	6.8	45.8	9.8	1.9 < 5	-
7	7	52.1	11.5	3.7 < 5	-
7 1/4	7.4	67.5	15.5	6.5	0.8 < 5
7 1/2	7.6	76.8	17.9	8	3.1 < 5
7 3/4	8	99.3	23.5	11.3	6
8	8.2	112.9	26.9	13.1	7.4

5. DETERMINISTIC SEISMIC HAZARD MAP

In **Fig.4**, the contours of median PRA (0.1g, 0.3g, 0.5g and 0.7g) resulting from MCE's are constructed based on the shortest horizontal distance from each seismogenic fault trace derived from Eq.(6). Less than 5 km distances are excluded in view of the accuracy of fault geometry, because the critical distance in the criteria for grouping active faults is 5 km. The highest PRA is set at 0.7g for engineering application.

It should be noted that only crustal earthquakes in Japan are considered in this study. As noted before, there can be some regions subjected more severely to deep seated and subduction earthquakes.

In this approach, the other fault parameters than fault length and geometry are not considered such as the dip angle of fault plane and the directivity of fault rupture. All seismogenic faults are assumed to be vertical faults. The fault rupture is assumed to release seismic energy uniformly around the fault plane.

Earthquake recurrence or probability of each seismogenic fault is not considered in this method. The PRA contours do not reflect probability or earthquake occurrence rate. Therefore, **Fig.4** is a conservative seismic hazard map with regard to the crustal shallow earthquakes. It will be useful for long-life critical structures or other civil structures which are often rehabilitated or retrofitted, and used in excess of their original design life for economical reasons.

Earthquake prediction consists of time, location, and magnitude factors. This deterministic seismic hazard map covers the last two factors of the three.

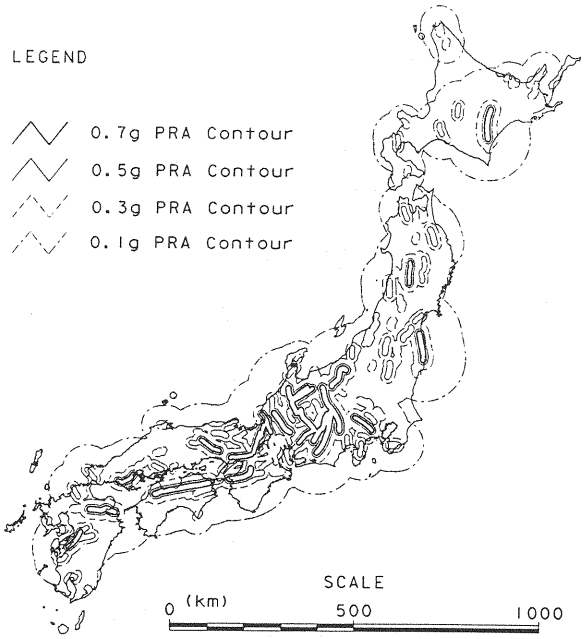

Fig.4 PRA contours from MCE's on land in Japan

It is based on some assumptions and simplifications, but is practical enough to design structures against crustal earthquakes.

Fig.5 shows seismic zoning map in the Japanese seismic design specifications for highway bridges[19]. Since the effects of the individual active faults on the Japanese islands are reflected in **Fig.4**, it may be of some help for re-estimating seismic hazard zoning and its zone factors after the Great Hanshin earthquake. It will also be useful for planning seismic retrofit strategy and seismic hazard prioritization.

6. COMPARISON OF DESIGN SEISMIC FORCES

The Caltrans' and Japanese approaches for seismic design are discussed briefly, followed by comparison of design seismic forces of the two methods. In the Caltrans' approach, PRA from the deterministic method has been used for scaling design seismic loads of highway bridges since 1974. For structures with well balanced spans and supporting bents of approximately equal stiffness,

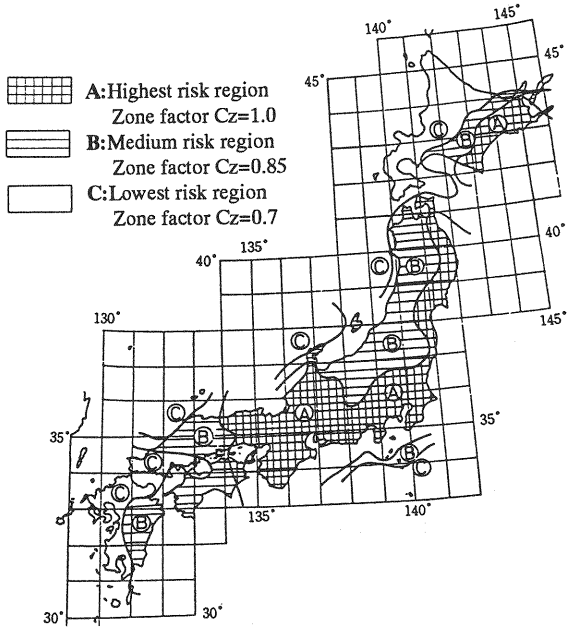

Fig.5 Regional classification of intensity of earthquake motion[19]

Caltrans uses the following procedures to calculate seismic member lateral forces in the equivalent static analysis method[20]:

$$E_Q = A\,R\,S\,W \qquad (9)$$

$$Z = -1.25T + 6.75 \quad (3 \geq T \geq 0.6)$$
$$6 \quad (0.6 > T) \qquad (10)$$

where, E_Q is the equivalent uniform static lateral load applied at the vertical center of gravity of the total structure, A (g) is the PRA ranging from 0.1g to 0.7g, R is the 5 % damped elastic acceleration response spectrum on rock normalized by PRA, S is the soil amplification spectral ratio for the site, W is the total dead load of the bridge, Z is the adjustment factor for ductility and risk assessment for well confined ductile single column bents, and T (sec) is the period of the structure. ARS means the 5 % damped elastic acceleration response spectrum at the site. The minimum value of ARS in the equivalent static analysis method is 0.4g. **Fig.6** shows ARS spectra for 3.0m-24.4m Alluvium Type for each level of PRA. E_Q is distributed to

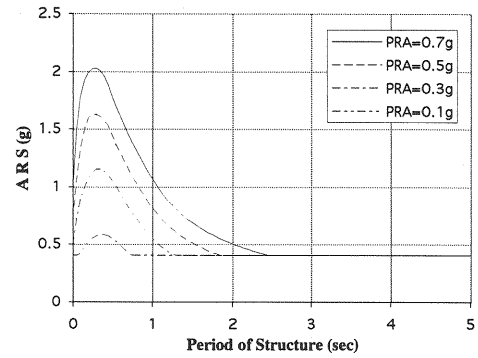

Fig.6 ARS spectra for the equivalent static analysis method (3.0m-24.4m Alluvium)

individual members according to the stiffness of the superstructure and supporting bents or piers.

Seismic forces are determined for two independent loading conditions in the longitudinal and transverse axis of the bridge. In order to account for directional uncertainty of earthquake motions, the forces resulting from the analysis of the two perpendicular seismic loading are combined into two load cases. In the first case, the forces from the transverse loading are combined with 30 % of the corresponding forces from the longitudinal loading. In the other case, the forces from the longitudinal loading are combined with 30 % of the corresponding forces from the transverse loading. Seismic design forces for individual members are determined by taking the distributed seismic member forces from the above two cases and dividing by Z.

In the Japanese approach, seismic lateral forces for design are calculated by the following design seismic coefficient (DSC) equation[19]:

$$k_h = c_z\, c_G\, c_I\, c_T\, k_{h0} \qquad (11)$$

$$c_T = 1.49T^{-2/3} \quad (1.3 < T)$$
$$1.25 \quad (1.3 \geq T \geq 0.2)$$
$$2.15T^{1/3} \quad (T < 0.2,\ c_T \geq 1) \qquad (12)$$

where, k_h is the horizontal DSC, c_z is the zone factor consisting of 3 zones, A, B, and C which are 1.0, 0.85, 0.7 respectively; c_G is the ground condition factor, 1.0 used here for Ground Condition Type 2; c_I is the importance factor, 1.0

used here for Class 1; c_T is the natural period factor for Ground Condition Type 2; T (sec) is the fundamental natural period of bridges; and k_{h0} is the standard horizontal DSC, 0.2. Equivalent static forces as seismic loads are obtained by multiplying the weight of design vibration unit by k_h, which is supposed to vibrate in the same manner during an earthquake.

An attempt is made to compare Caltrans' and Japanese design seismic forces in a particular, simple case. The following assumptions are made for the comparison:

1) The site condition in this case falls into both Caltrans' 3.0m-24.4m Alluvium Type and Japanese Ground Condition Type 2.

2) The combination of the longitudinal and transverse loading in the Caltrans' method is not considered here.

3) The structure has well balanced spans and single column bents with approximately equal stiffness. A seismic load distributed to each column is an equivalent uniform load.

Under the above assumptions, Caltrans' ARS/Z is compared directly with Japanese DSC. ARS/Z and DSC for a single column in the highway bridge specifications are compared for each level of the seismic hazard in **Fig.7**. ARS/Z values are of wider range from 0.07 to 0.34, which means they are more sensitive to both the seismic hazard and the period of structure. For periods less than 1 second, Caltrans has higher coefficients for the 0.5g and 0.7g PRA curves, while Japan has higher DSC's in general. Therefore, Caltrans' design seismic loads for structures with short periods are more conservative in the near-field areas with 0.5g or higher PRA seismic hazard in this particular case. If highway bridge structures are designed in Japan according to the Caltrans' specifications, the design seismic load to the short-period structures will be higher in the 0.5g and 0.7g areas in **Fig.4** on the above assumptions. The experience of the Great Hanshin earthquake suggests the high risk areas in **Fig.4** be taken into consideration in the future Japanese specifications.

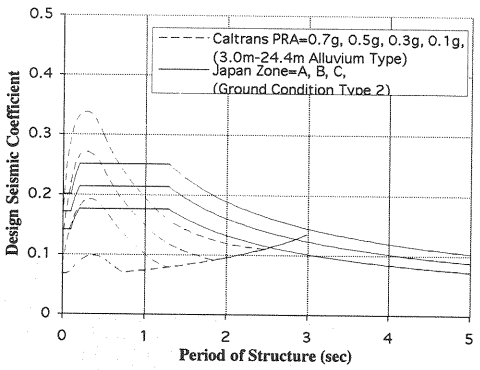

Fig.7 Comparison of design seismic coefficients for a si ngle column bent

7. CONCLUSION

A deterministic seismic hazard map of Japan based on MCE's from inland seismogenic faults is presented. Since seismic hazard is estimated regardless of occurrence probability, even active faults with long recurrence, such as one thousand years, are included automatically in this map. It will be appropriate for evaluating seismic loads for long-life and important structures.

This map will be helpful for estimating the seismic hazard zoning and its zone factors in the current Japanese specifications for highway bridges, because the individual active faults are taken into account there. It will also be useful for planning of seismic retrofit strategy.

Since only inland seismogenic faults are used as seismic sources, it should be noted that some regions may be more affected by large deep subduction and other deep seated earthquakes. Such effects should be incorporated in this map or another map for them should be made in the future.

The comparison of Caltrans' and Japanese design seismic loads in a particular case shows that Caltrans use more conservative seismic loads for bridges with short periods in the near-field regions with 0.5g or higher PRA seismic hazard.

ACKNOWLEDGMENT: We want to express our thanks to the support of Caltrans and Hanshin Expressway in preparing this paper. Also we had the benefit of getting valuable advice from many people, both from the United States and Japan. In particular, Prof. Matsuda of Kumamoto University provided excellent ideas for geologic information.

REFERENCES

1) Matsuda, T.: Seismic zoning map of Japanese islands with maximum magnitudes derived from active faults data, *Bull. Earthq. Res. Inst., Univ. Tokyo*, Vol.65, pp.289-319, 1990. (in Japanese)
2) Architectural Institute of Japan: *Preliminary Reconnaissance Report of the 1995 Hyogoken-Nanbu Earthquake*, 1995.
3) Omote, S., Ohsaki, Y., Kakimi, T. and Matsuda, T.: Japanese practice for estimating the expected maximum earthquake force at a nuclear power plant site, *Bull. New Zealand Nat. Soc. Earthq. Eng.*, Vol.13, pp.37-48, 1980.
4) Kameda, H. and Okumura, T.: Seismic hazard estimation based on active fault data and historical earthquake data, JSCE Journ. Struc. Mecha. Earthq. Eng., Vol.362/I-4, pp.407-415, 1985. (in Japanese)
5) Mualchin, L. and Jones, A.L.: Peak acceleration from maximum credible earthquakes in California (rock and stiff soil sites), California Depart. Consev., Div. Mines and Geol. Open-File Repo. 92-1, 1992.
6) Research Group for Active Faults: *Active faults in Japan, Sheet maps and inventories*, Univ. of Tokyo Press, 1980. (in Japanese)
7) Research Group for Active Faults: *Active faults in Japan, Sheet maps and inventories, revised edition*, Univ. of Tokyo Press, 1991. (in Japanese)
8) Bonilla, M.G., Mark, R.K. and Lienkaemer, J.J.: Statistical relations among earthquake magnitude, surface rupture length and surface fault displacement, *Bull. Seism. Soc. Amer.*, Vol.74, pp.2379-2411, 1984.
9) Matsuda, T.: Magnitude and recurrence interval of earthquakes from a fault, *Jisin Journal*, Seism. Soc. Japan, Vol.28, No.3, pp.269-283, 1975. (in Jap anese)
10) Campbell, K.W.: Near-source attenuation of peak horizontal acceleration, *Bull. Seism. Soc. Amer.*, Vol.71, No.6, pp.2039-2070, 1981.
11) Campbell, K.W.: Strong motion attenuation relations: a ten-year perspective, *Earthq. Spectra*, Vol.1, No.4, pp.759-804, 1985.
12) Annaka, T. and Nozawa, Y.: A probabilistic model for seismic hazard estimation in the Kanto district, *Proc. 9th World Conf. Earthq. Eng.*, Vol.2, pp.107-112, 1988.
13) Fukushima, Y. and Tanaka, T.: A new attenuation relation for peak horizontal acceleration of strong earthquake ground motion in Japan, *Bull. Seism. Soc. Amer.*, Vol.80, No.4, pp.757-783, 1990.
14) Boore, D.M., Joyner, W.B. and Fumal, T.E.: Estimation of response spectra and peak accelerations from western north American earthquakes: an interim report, U.S. Geol. Surv. Open-file Report 93-509, 1993.
15) Molas, G.L. and Yamazaki, F.: Attenuation of earthquake ground motion in Japan including deep focus events, *Bull. Seism. Soc. Amer.*, Vol.85, No.5, pp.1343-1358, 1995.
16) Molas, G.L. and Yamazaki, F.: Attenuation of ground motion during the 1995 Great Hanshin Earthquake, *Bull. Earthq. Resist. Struct.*, Inst. Indus. Sci., Univ. of Tokyo, No.28, pp.25-41, 1995.
17) Ansary, M.A., Yamazaki, F. and Katayama, T.: Peak values of ground motion indices based on two horizontal components, *Proc. 9th Japan Earthq. Eng. Symp.*, Vol.3, pp.E37-E42, 1994.
18) Utsu, T.: Relationships between earthquake magnitude scales, *Bull. Earthq. Res. Inst.*, Univ. Tokyo, Vol.57, pp.465-497, 1982. (in Japanese)
19) Japan Road Association: *Specifications for highway bridges*, Part V: Seismic design, 1990.
20) California Department of Transportation: *Bridge Design Specifications*, Div. 1-Design, Sec. 3-Loads, 1990.

(Received August 19, 1996)